Tight Junction Structure and ZO-1 Content Are Identical in Two Strains of Madin–Darby Canine Kidney Cells Which Differ in Transepithelial Resistance

Bruce R. Stevenson,* James Melvin Anderson,‡ Daniel A. Goodenough,§ and Mark S. Mooseker*‖

* Department of Biology, Yale University, ‡ Department of Medicine and Liver Center, and ‖ Department of Cell Biology, Yale University School of Medicine, New Haven, Connecticut 06511; and § Department of Anatomy and Cellular Biology, Harvard Medical School, Boston, Massachusetts 02115.

Abstract. The relationship of tight junction permeability to junction structure and composition was examined using two strains of Madin-Darby canine kidney (MDCK) cells (I and II) which differ > 30-fold in transepithelial resistance. This parameter is largely determined by paracellular, and hence junctional, permeability under most conditions. When these two strains of cells were grown on permeable filter supports, they formed monolayers with equivalent linear amounts of junction/area of monolayer. Ultrastructural analysis of these monolayers by thin section EM revealed no differences in overall cellular morphology or in tight junction organization. Morphometric analysis of freeze-fractured preparations indicated that the tight junctions of these two cell strains were similar in both number and density of junctional fibrils. Prediction of transepithelial resistance for the two strains from this freeze-fracture data and a published structure-function formulation (Claude, P. 1978. *J. Memb. Biol.* 39:219–232) yielded values (I = 26.5 Ω/cm², II = 35.7 Ω/cm²) that were significantly lower than those observed (I = 2,500–5,000 Ω/cm², II = 50–70 Ω/cm²). Consistent with these structural studies, a comparison of the distribution and cellular content of ZO-1, a polypeptide localized exclusively to the tight junction, revealed no significant differences in either the localization of ZO-1 or the amount of ZO-1 per micron of junction (I = 1,415 ± 101 molecules/μm, II = 1,514 ± 215 molecules/μm).

THE *zonula occludens*, or tight junction, plays a critical role in epithelial cell biology (see references 3, 20, 24, 36, 38 for review). It forms a selectively permeable occlusion in the paracellular pathway, thereby defining apical and basal compartments, and is thought to be at least partially responsible for the maintenance of membrane compositional asymmetry.

Structurally, the tight junction has been well-defined. It appears in thin section as a series of individual contacts between the plasma membranes of adjacent epithelial cells (11). These points of contact correspond in freeze-fracture to a variably complex network of fibrils lying within the plane of the plasma membrane (19, 22).

The structural elements responsible for controlling junctional permeability remain unknown. A hypothesis has been proposed that states that junctional permeability is inversely proportional to the mean number of freeze-fracture fibrils seen along the apical-basolateral axis (7, 8). While exceptions to this rule have been cited (12, 17, 31, 32, 33), careful analysis has demonstrated that tight junctions in various tissues are both morphologically and physiologically heterogeneous (5, 27) and, when treated as a circuit of parallel resistors, appear to conform to the original structure-function relationship (25, 30). Indirect evidence indicates that permeability may be influenced by cytoskeletal elements found in close approximation to the junction (23, 26, 28, 29).

Tight junction physiology can be assessed, in part, by measuring transepithelial resistance. Because the resistances of the epithelial plasma membranes are, in most circumstances, relatively so high, transepithelial resistance reflects the resistance to current flowing through the tight junction and hence its ionic permeability (7, 9, 10, 13). Junctional permeability varies depending upon both the type of epithelium and the surrounding external environment (4, 7).

To fully characterize the tight junction, it is also necessary to define the molecular components of the junction, their relationships to each other, and their interactions with nonjunctional cellular structures. ZO-1, a polypeptide of 225 kD in hepatocytes, is the first component exclusively localized to the tight junction in a variety of mature epithelial and endothelial cells, including the MDCK cell line (39). This protein has been shown to be phosphorylated at serine residues and behaves in hydrodynamic analyses as an elongated monomer (1). ZO-1 is peripherally associated with the junctional membrane and present in approximately the same quantities as the intramembranous particles that make up the

freeze-fractured tight junctional fibrils (1). Recently, an additional tight junction-associated component, termed "cingulin," has been identified and purified from chicken intestinal brush borders (6). Although cingulin is also an elongated, peripheral membrane protein (6), it is immunologically distinct from ZO-1 (Stevenson, B, and S. Citi, unpublished observations). There is no direct information, however, on the relationship of either ZO-1 or cingulin to tight junction physiology or structure.

The Madin-Darby canine kidney (MDCK) epithelial cell line offers an advantageous system for studying tight junction structure and function. This cell line forms an epithelial monolayer in culture which contains functionally intact tight junctions (4). More importantly, two strains of MDCK cells have been identified which exhibit a number of functional and biochemical differences, including a striking disparity in transepithelial resistance. Strain I monolayers have a resistance of $\sim$3,000 Ω/cm^2, while strain II cells typically display values of 50–100 Ω/cm^2 (14, 34, 40). Both strains of cells can readily be grown on permeable filters, allowing cells to feed from their basolateral surfaces, a condition much more like that found in situ (15, 36). These growth conditions also permit direct coanalysis of transepithelial resistance and tight junction structural and compositional characteristics.

We report here a comparison of various parameters of the tight junctions of these two strains of MDCK cells grown on permeable substrates. Contrary to previous studies which have related the number of tight junction freeze-fracture fibrils to transepithelial resistance (7, 8, 25, 30), we observed no structural differences in the tight junctions of these two cell strains. Nor did we observe a difference in the distribution or content of the tight junction-associated protein ZO-1. The significance of these results is discussed in the context of current models for the regulation of tight junction permeability.

Materials and Methods

All reagents were purchased from Sigma Chemical Co. (St. Louis, MO) unless otherwise indicated.

Cell Culture

MDCK cells were grown on uncoated plastic or glass coverslips as described previously (39) in either DME or MEM with Earl's salts (Hazleton Biologics Inc., Lenexa, KS) supplemented with 10 mM Hepes (Research Organics, Inc., Cleveland, OH).

Cells were also grown on polycarbonate filter inserts (model No. 3412; Costar Data Packaging Corp., Cambridge, MA). MDCK I cells were plated at 1-2 $\times$ 10^5 cells/cm^2 and allowed to incubate for 4 d to achieve maximal transepithelial resistance (21). MDCK II cells were plated at 2-3 $\times$ 10^5 cells/cm^2 and used 2-3 d later (35). Plating densities and times of incubation were chosen to produce confluent monolayers of optimal transepithelial resistance. Filters from both strains were suspended off the bottom of 150 $\times$ 25-mm petri dishes (Nunc, Inc., Naperville, IL) by sterile lexan plastic inserts designed to hold five filters per petri dishes (Costar Packaging Corp.). The petri dish (basal compartment) contained 75 ml of medium, while the cells were plated in the interior (apical compartment) of the filter insert in 2 ml of medium/filter.

Electrophysiology

Transepithelial resistance was determined by passing a known current across the monolayer and measuring the resultant voltage deflection. Current pulses of 10–100 μA and of $\sim$1 s duration were generated by a constant current stimulator (Electronics for Life Sciences, Rockville, MD) between two Ag/AgCl electrodes (E. M. Wright, Guilford, CT). Induced voltage was measured between pairs of matched calomel electrodes (Fisher Scientific Co., Pittsburg, PA) with a VF-1 oscilloscope (Tektronix, Inc., Beaverton, OR). Electrodes were connected to the cell monolayer solution via salt bridges composed of 3% agar (Difco Laboratories, Inc., Detroit, MI) in Dulbecco's PBS (DPBS[1]; 137 mM NaCl, 2.7 mM KCl, 0.9 mM $CaCl_2$, 0.5 mM $MgCl_2$, 8 mM Na_2HPO_4, 1.5 mM KH_2PO_4, pH 7.4) without the Ca^{2+} or Mg^{2+}. Before measurements electrodes were short circuited to allow equilibration.

Filters containing cell monolayers were removed from the culture incubator and immediately rinsed with DPBS ($+Ca^{2+}$, $+Mg^{2+}$) at 37°C. Measurements were made in DPBS and transepithelial resistance calculated taking into account the resistance of a similarly treated blank filter. Filters were then placed on ice for further processing.

Electron Microscopy

Thin Section. Monolayers of known transepithelial resistance were fixed in 2% glutaraldehyde (Polysciences, Inc., Warrington, PA) in 0.1 M phosphate, pH 7.0 for 15 min, followed by 2% glutaraldehyde, 0.1 M phosphate, pH 7.0, containing 0.2% tannic acid (Mallinckrodt Inc., St. Louis, MO) for 15 min. Cells were postfixed in 1% OsO_4 (Electron Microscopy Sciences, Fort Washington, PA) in 0.1 M phosphate, pH 6.0 for 20 min and en bloc stained with aqueous 1% uranyl acetate (Fisher Scientific Co.) for 20 min. Sections were stained with lead citrate and viewed in a Zeiss EM 10C electron microscope operating at 80 kV (Carl Zeiss, Inc., Oberkochen, West Germany).

Freeze-Fracture. 20 filters of each MDCK strain whose transepithelial resistance was previously determined were fixed in 2.5% glutaraldehyde, 2% paraformaldehyde/2% glutaraldehyde, or 1% paraformaldehyde/1% glutaraldehyde in 0.1 M sodium cacodylate, pH 7.4 for 30 min on ice. Immediately before freezing the fixed monolayers were equilibrated in 20% glycerol (Fisher Scientific Co.) in 0.1 M sodium cacodylate, pH 7.4. Monolayers were scraped from the filter using a rubber policeperson, pelleted gently in a table-top clinical centrifuge (International Equipment Co., Needham Heights, MA), and a slurry of the cell pellet applied to gold, double replica hats (Balzers High Vacuum Corp., Nashua, NH). Samples were frozen in liquid nitrogen-cooled freon, fractured in a freeze-fracture device (model No. BAF301; Balzers High Vacuum Corp.), and shadowed with platinum-carbon. Replicas were examined in the Zeiss electron microscope and regions containing tight junctions were photographed at 20,000×. A standard calibration grid (2,160 lines/mm; Ernest F. Fullam, Inc. Schenectady, NY) was used to verify microscope magnification.

Fibril counts were made on freeze-fracture micrographs according to the procedure of Claude and Goodenough (1973). A perpendicular line was drawn on junctions every 0.5 μm and the number of fibrils intersecting that line counted. On junctions whose length was >0.5 μm, network density, the total length of junctional fibrils divided by the overall length of apical surface bordered by the junction (32), was also measured by tracing the individual fibrils with an electronic graphics calculator (Numonics Corp., Lansdale, PA).

Prediction of transepithelial resistances for the two MDCK strains was performed to test the structure-function relationship described by Claude and Goodenough (1973) and Claude (1978). The resistance of a junction of a given fibril number can be calculated from Claude's graph of $R_j I_p$ (R_j = junctional resistance, I_p = linear junctional density) vs. fibril number (Fig. 4. of reference 7). Corrected for the linear junctional density for each MDCK strain, the predicted resistances can then be inserted into the equation describing the total resistance of a circuit of parallel resistors (25, 30):

$$1/R_T = f_1/R_1 + f_2/R_2 + f_3/R_3 + \ldots$$

where R_T = total resistance; f_n = frequency of appearance of a given fibril number (our Fig. 4); and R_n = the resistance of that fibril number determined from Claude's graph. The predictions assume that R_j is equivalent to transepithelial resistance.

Antibodies

The anti-ZO-1 mAbs R26.4 and R40.76 generated against a tight junction-enriched preparation from mouse liver (37) were used exclusively in this study and have been previously described (1, 39). R40.76 antibodies were coupled to Sepharose (Pharmacia Fine Chemicals, Uppsala, Sweden)

1. *Abbreviation used in this paper*: DPBS, Dulbecco's PBS.

according to manufacturer's protocol and used to immunoprecipitate ZO-1 according to the method of Anderson et al. (1988).

Light Microscopy

Glass coverslips containing confluent monolayers of MDCK cells were rinsed once with DPBS, fixed with 2.5% paraformaldehyde (Polysciences, Inc.) in DPBS for 30 min on ice, quenched with 0.5 mg/ml sodium borohydride, and permeabilized with −20° methanol for 4 min. Monolayers were stained with either enriched serum-free culture supernatant used undiluted (39) or ascites fluid produced against the hybridomas in athymic mice (1) diluted 1:100 in TBS (150 mM NaCl, 10 mM Tris, pH 7.4), followed by fluorescein-conjugated rabbit anti-rat secondary antibodies (Boehringer Mannheim Biochemicals, Indianapolis, IN). Filter-grown monolayers were similarly treated except that a 1-cm^2 piece of the polycarbonate filter was cut from the filter chamber before methanol permeabilization. Before light microscopic examination the filter pieces were sandwiched between a glass slide and coverslip in mounting medium (60% glycerol/TBS, 0.4% *n*-propyl gallate).

Microscopy was performed on a Zeiss light microscope equipped with a 63× planapo objective. Photographs were taken on Tri-X film (Eastman Kodak Co., Rochester, NY). Morphometric analysis was done on photographs of MDCK I and II monolayers immunofluorescently stained for ZO-1. Linear junctional density (the linear amount of junction/monolayer area; reference 7) was determined by tracing the ZO-1 staining using the integrating planimeter (Numonics Corp.). Cell densities were calculated by counting the cells on the same photomicrographs.

Quantification of ZO-1

The amount of ZO-1 present in monolayers of each strain of MDCK cell was determined by competitive and saturable binding of radiolabeled mAbs (R40.76) to MDCK total cell protein immobilized on nitrocellulose paper. Filter-grown monolayers whose transepithelial resistance was previously determined were solubilized in 10 mM Tris, 0.1% SDS, pH 7.4. Aliquots of this total cell protein suspension were then applied to nitrocellulose paper and the ZO-1 quantified according to a procedure described previously (1).

Results

Ultrastructural Analysis

MDCK I and II cells grown on permeable filter supports were indistinguishable from each other in thin section electron microscopy (Fig. 1). They had a typical cuboidal epithelial morphology, were of uniform height, and had stubby microvilli sparsely decorating their apical surfaces. Immediately subjacent to their basal plasma membrane was a thin, wispy basal lamina with very little indigitation of cellular processes into the polycarbonate filter pores (Fig. 1, *inset*). The lateral cell surfaces showed a variable degree of membrane infolding, and the junctional complexes were located at the intersection of the lateral and apical membrane domains. Typical desmosomes were found randomly distributed along the entire lateral cell surface, and the *zonula adherens* was less pronounced than in some other epithelial cell types (e.g., intestinal epithelial cells). The tight junction was found at the apical-most aspect of the lateral cell surface. It was composed of a variable number of membrane contacts with no organized pattern of cytoskeletal elements discernable in the adjacent cytoplasm. There were no consistent differences between the two cell strains in any aspect of tight junctional anatomy, including junctional height. Similar morphological characteristics were previously reported for MDCK II cells grown on permeable substrates (4).

Previous quantification of freeze-fracture images from a variety of epithelia lead to the hypothesis that there is a direct logarithmic relationship between transepithelial resistance and the number of tight junctional fibrils (7, 8). Given

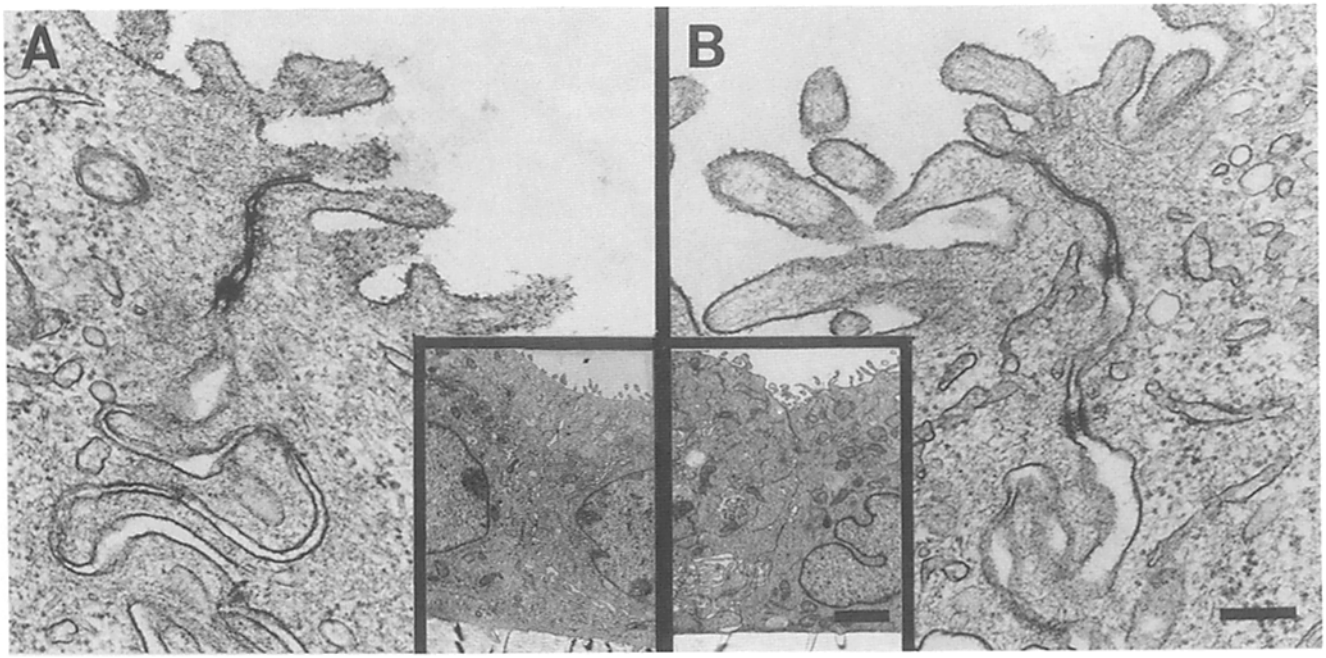

Figure 1. Thin section electron microscopic comparison of MDCK I and II cells grown on filters. (*A*) MDCK I cell junctional complex region. (*B*) Similar region in MDCK II cell. No consistent differences in any morphological characteristic were observed in either cell strain, including tight junction structure. Insets show low magnification view of the MDCK monolayers showing their overall similarity in height, degree of lateral surface infolding, and other structural properties. At the bottom of each the polycarbonate filter is visible. Bar, 200 nM; inset bar, 2 μM.

the large difference in the transepithelial resistance of the MDCK I and II cell strains, the high resistance strain I cells should, according to this theory, display a significantly higher number of freeze-fracture fibrils. However, upon examination it was found that freeze-fractured tight junctions from these two strains of cells grown on permeable substrates appeared identical (Fig. 2). Both the high resistance strain I (Fig. 2, *A* and *C*) and the low resistance strain II (Fig. 2, *B* and *D*) exhibited similar branching and anastomosing patterns of fibrils lying with the P fracture face, with corresponding grooves in the E fracture face. Using a variety of fixation conditions, there was also no consistent difference in individual fibril morphology (data not shown).

To quantitatively evaluate these freeze-fracture images, the mean fibril number was determined by making numerous counts along a line drawn perpendicular to the junctional axis (see Materials and Methods). Network density, a measure of the complexity of the fibril branching pattern (32), was also determined. These measurements confirmed that there was no significant difference in either parameter between MDCK I and II cells (Table I). Potential heterogeneity in the mean fibril number counts could be revealed by displaying the data in the form of a histogram (Fig. 3). Contrary to the structure-function hypothesis (7, 8), it appeared that while the two strains display similar fibril number distributions, the low resistance strain II junctions actually tended toward having a greater number of junctions with a high number of fibrils.

Knowledge of the frequency of observation of the various fibril numbers, together with the linear junctional densities of the MDCK I and II monolayers, allowed predictions to be made of the transepithelial resistance for each strain based on the previously described structure-function relationship (7, 8; see Materials and Methods). The freeze-fracture data

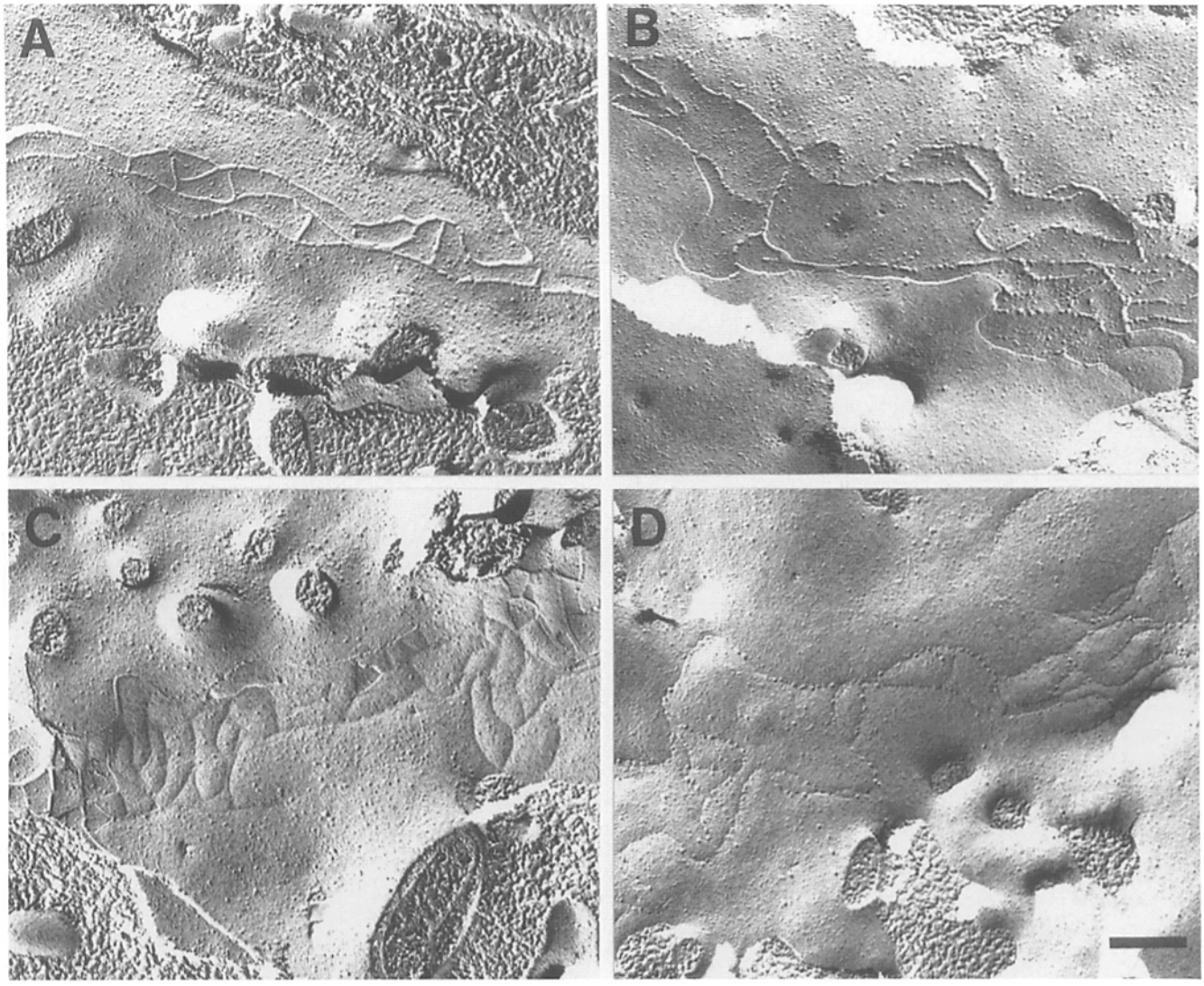

Figure 2. Freeze-fracture replicas of filter-grown MDCK I and II cell surfaces providing views of the tight junction. The tight junction displays a branching network of P-face fibrils (*A* and *B*) and corresponding E-face grooves (*C* and *D*) running in the plane of the membrane at the interface of the apical and lateral membrane domains. (*A* and *C*) MDCK I cells. (*B* and *D*) MDCK II cells. Both strains of MDCK cells show similar fibril numbers and branching complexity. The more discontinuous morphology seen in the MDCK II fibrils (compare *A* with *B*) was not a consistent observation. Bar, 200 nM.

Table I. Freeze-Fracture Quantification

	MDCK I	MDCK II
Fibril number	3.9 ± 1.4 (168)*	4.7 ± 2.2 (78)
Network density‡	4.3 ± 1.4 (42)	6.6 ± 2.4 (25)
Transfilter resistance§ (Ω/cm^2)	4492 ± 2554 (19)	55 ± 28 (23)

* Mean ± standard deviation (*n*).
‡ Total fibril length per length of apical surface bordered by ZO (32).
§ Resistance of filters used for freeze-fracture analyses.

obtained in the MDCK I and II cells predicted resistances of 26.5 Ω/cm^2 for strain I MDCK cells and 35.7 Ω/cm^2 for strain II cells.

Determination of ZO-1 Distribution and Content

Light Microscopic Immunolocalization of ZO-1. MDCK I and II cells grown on impermeable substrates such as glass or plastic produced a dissimilar immunofluorescence pattern when stained with anti-ZO-1 monoclonal antibodies (Fig. 4, *A* and *B*). While both cell types showed the typical discrete localization of ZO-1 at the junctional region of the cell periphery, ZO-1 staining in MDCK II cells had a more clumped or broken appearance. The possibility that this appearance was produced by the junction moving up or down out of the plane of focus rather than by actual discontinuities could not be resolved by optical sectioning. MDCK I cells also appeared to be larger and more irregularly shaped than the MDCK II cells on impermeable substrates. When grown on permeable filter supports, the cells were not only approximately the same size and shape, but also more densely packed than those grown on plastic or glass (Fig. 4, *C* and *D*). However, the apparent discontinuities in ZO-1 staining were still visible in filter-grown MDCK II monolayers.

Determination of the linear junction density, the linear amount of junction in a given area of monolayer (7), as well as the cell density for confluent MDCK I and II cell monolayers grown on both types of substrates and stained for ZO-1 activity verified these observations (Table II). The low resistance strain II cells showed significantly higher cell and linear junctional densities when incubated on impermeable surfaces. However, on filters, MDCK I cells showed slightly higher values for both parameters. Both cell types formed more densely packed monolayers on filters, as compared to plastic or glass.

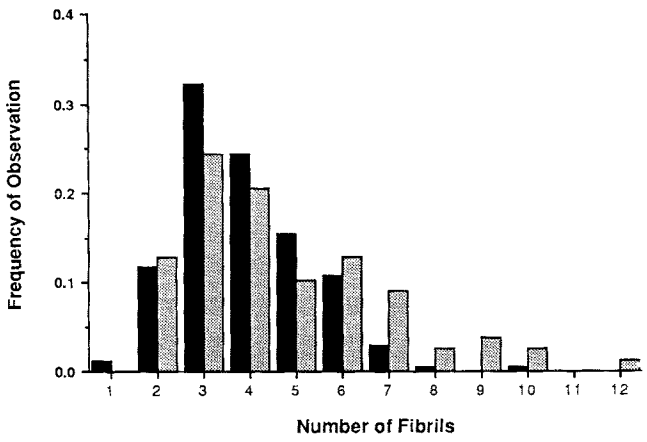

Figure 3. Histogram comparing the frequency of observation of a given number of fibrils in MDCK I (*solid bars*) and MDCK II (*stippled bars*) cell freeze-fracture replicas. Both cell strains show a similar distribution, but with MDCK II cells having slightly more junctions with a higher number of fibrils. ■, MDCK I; ▨, MDCK II.

Quantification of ZO-1. The amount of ZO-1 present in each strain of MDCK cell was assayed by solubilizing confluent monolayers of cells on filters and quantitating the binding of radioactively labeled anti-ZO-1 antibodies to total soluble protein immobilized on nitrocellulose paper (reference 1; Table III). The results demonstrated that there was an equivalent amount of ZO-1 present in each cell strain (I = 1,415 ± 101 molecules of ZO-1/μm of junction, II = 1,514 ± 215 molecules/μm).

Discussion

MDCK I and II cell strains show a large difference in transepithelial resistance, possibly related to their derivation from different areas of the kidney (34). There are several possible explanations for this difference, based on the assumption that transepithelial resistance values are reflective of tight junctional permeability. The junctions themselves could display structural differences, either in the form of an increase in the number of fibrils, as suggested by previous reports (7, 8), or in discontinuities in either the junctions or fibrils themselves. One monolayer could contain a higher linear amount of junction per area than the other. Assuming that the junctions themselves have the same resistance, having more junction per area would result in lower transepithelial resistance measurements. As discussed below, the results presented in this report do not support any of these possibilities.

The ultrastructural studies presented here (Figs. 1 and 2, and Table I) indicate that the difference in transepithelial resistance observed for MDCK strains I and II monolayers is not due to obvious differences in cell morphology or in the structural organization of their tight junctions. In particular, the freeze-fracture analysis of tight junction structure in these two cell strains failed to reveal any significant differences in fibril number or complexity. Similar morphometric results from two separate MDCK cell clones have been reported in preliminary form (Gonzalez-Mariscal, L., B. Chavez de Ramirez, G. Avila, and M. Cereijido, unpublished observations).

The thin section EM morphology of both cell strains was similar to that previously reported for MDCK II cells (4). In another thin section EM comparison Richardson et al. (1981) found that MDCK II cells are taller and have longer and more densely packed microvilli than MDCK I cells. However, these observations were made on cells grown on Millipore nitrocellulose filters (as opposed to the Costar polycarbonate filters used in this study), and MDCK cells have been shown to display different characteristics depending on growth substrate composition (40).

Anderson et al. (1988) previously observed that the amount of ZO-1 in MDCK cells is roughly equivalent to the average number of junctional fibril intramembranous particles seen in freeze-fracture. The equivalence in the content of ZO-1 in these two cell strains (Table III) provides additional evidence that these cells do not significantly differ in either the amount or complexity of their tight junctions. The

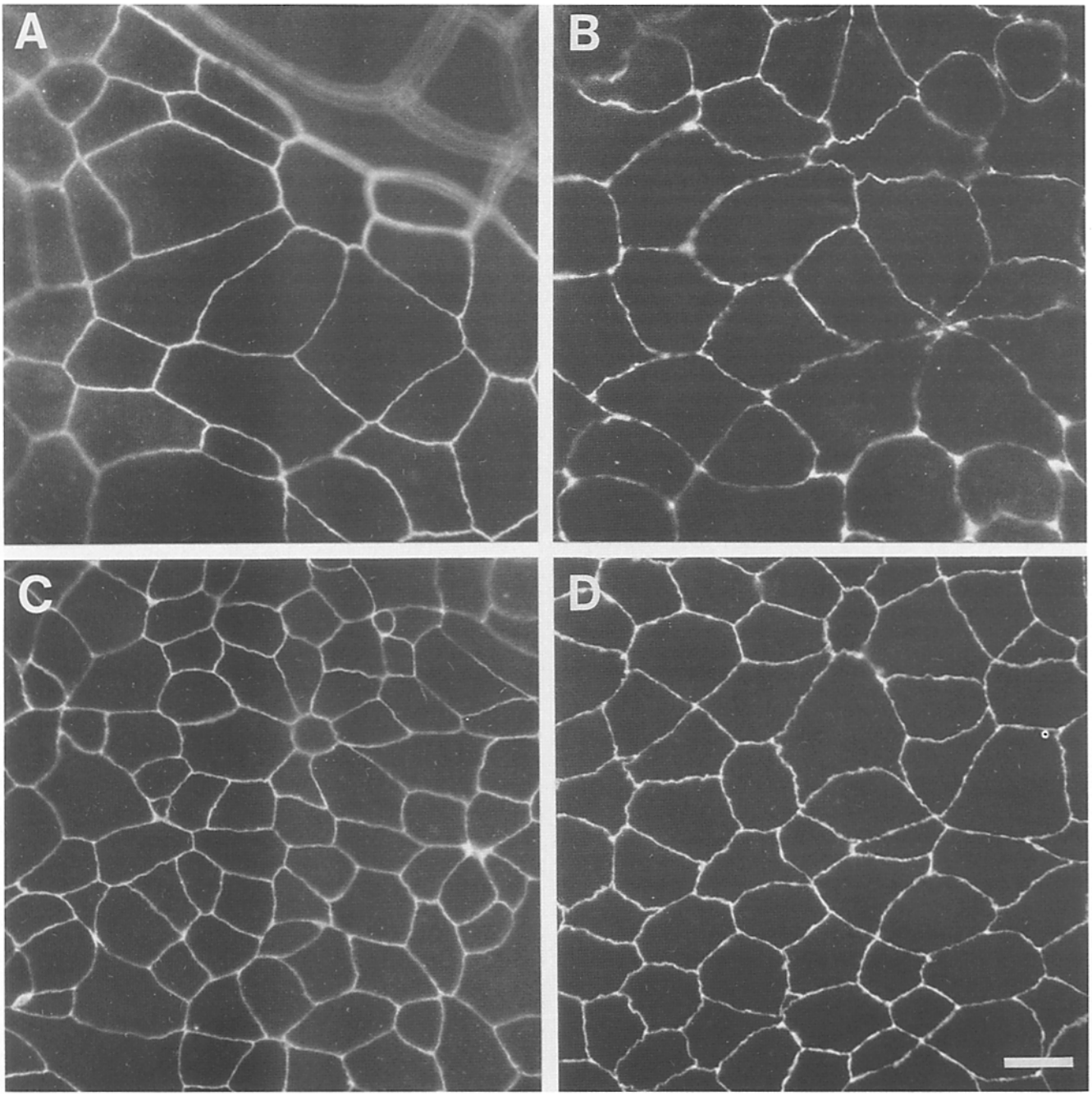

Figure 4. Immunofluorescent localization of ZO-1 in MDCK I and II monolayers using anti–ZO-1 mAbs. Discrete staining is visible in all cells at the level of the tight junction. (*A*) MDCK I cells grown on plastic. Cells are of irregular size and shape. (*B*) MDCK II cells grown on plastic. Cells are of more uniform shape and size, but ZO-1 staining appears more clumped or discontinuous. In both strains of cells on plastic the monolayers move up or down out of the plane of focus, an indication of dome formation. (*C*) MDCK I cells grown on Costar filters. Cells are more uniform in shape and smaller in cross section than those grown on plastic. (*D*) MDCK II cells on filters. These cells are also smaller, but the discontinuous staining pattern persists. Bar, 10 μM.

expression of ZO-1 content in terms of molecules of ZO-1 per micron of junction assumed that all of the ZO-1 present in these cells is located at the junctional membrane. This assumption was supported by the immunofluorescence observations. It is interesting that the values obtained here for molecules of ZO-1 per micron of junction were about twice that observed in the same cells grown on plastic (1). Since there was little difference in the average number of fibrils seen in freeze-fracture of either plastic- or filter-grown cells (18; Table I), this indicated that there is twice as much ZO-1 as fibril particles under these conditions. The meaning of this increase in ZO-1 content is unclear, although it may be reflective of a more fully differentiated junction resulting from growth on permeable substrates.

Table II. Comparison of Cell and Linear Junctional Densities of MDCK I and II Cells Grown on Permeable and Nonpermeable Substrates

	Substrate	MDCK I	MDCK II
Linear junctional density (m/cm²)	NP*	12.5 ± 1.9 (8)‡	16.6 ± 0.7 (8)
	P	21.0 ± 0.7 (13)	19.1 ± 0.5 (13)
Cell density (cells/cm² × 10^5)	NP	4.7 ± 0.9 (8)	7.2 ± 0.7 (8)
	P	13.0 ± 1.0 (10)	10.0 ± 1.0 (10)
Transfilter resistance§ (Ω/cm²)		2496 ± 598 (4)	65 ± 23 (4)

* NP = nonpermeable (plastic, glass); P = permeable (Costar filter).
‡ Mean ± standard deviation (*n*).
§ Resistance of filters used for density analyses.

As noted above, another possible way to achieve differences in transepithelial resistance would be to increase the linear amount of junction per area of monolayer. In fact, the high resistance MDCK I cells had slightly higher values of linear junctional density (Table II), the opposite of what one might expect. These measurements were done on light micrographs, so it was possible that simple tracing of ZO-1 staining may not have resolved micro-variations in junctional tortuousity. This seems unlikely, since both cell strains contain similar amounts of ZO-1 per junctional length (Table III). On the other hand, the low resistance of the MDCK II cells could be explained by the discontinuous immunofluorescence staining pattern observed in Fig. 4. A small number of openings in the tight junction could account for a large difference in transepithelial resistance (14). However, we feel this is an unlikely explanation. A second distinct clone of MDCK II cells (provided by Karl Matlin, Department of Anatomy and Cellular Biology, Harvard Medical School) with a transepithelial resistance similar to those used in this study showed no such discontinuities in the ZO-1 staining pattern (data not shown). In any event, none of this information explains why the MDCK I cells had such a high transepithelial resistance relative to their number of junctional fibrils.

Taken together, the structural and compositional results presented here indicate that a simple application of the structure-function hypothesis of Claude and Goodenough (1973), and Claude (1978) can not explain the observed differences in transepithelial resistance. This hypothesis can be partially tested by using the fibril data to predict transepithelial resistance. The values obtained from relating the number of fibrils to resistance from Calude's graph, together with linear junctional density and observation frequency in a circuit analysis (see Materials and Methods), were MDCK I = 26.5 Ω/cm² and MDCK II = 35.7 Ω/cm². However, this analysis did not take into account an additional factor described by Claude (1978); that of the probability of a hypothetical "pore" or channel in the junctional fibrils being open or closed. As this probability decreases, the transepithelial resistance increases logarithmically.

Table III. Quantification of ZO-1 MDCK I and II Cells

	MDCK I	MDCK II
Quantity of ZO-1 (molecules/μm of junction)	1415 ± 101 (8)*	1514 ± 215 (8)
Transfilter resistance‡ (Ω/cm²)	4940 ± 859 (8)	52 ± 34 (8)

* Mean ± standard deviation (*n*).
‡ Resistance of filters used for quantification of ZO-1.

It is possible that the two strains of MDCK cells have very different channel characteristics, accounting for the vast difference in resistance measurements (16). Since flux measurements indicate that junctional channels are impermeable to molecules with a hydrodynamic radius greater than 15Å (25, 28), one could not expect to resolve channel differences with the freeze-fracture technique. Also, as freeze-fracture splits the membrane bilayer, the structures responsible for permeability may not be revealed since they must be on the outside surface of the membrane (2). The analysis of Claude and Goodenough (1973) was also done on natural epithelia. The examination of transformed cell lines presented here may have introduced additional factors not previously considered. A clear understanding of this situation relies on the eventual identification and molecular analysis of the structural element responsible for the junctional permeability properties.

It is also possible that the difference in transepithelial resistance observed in these two cell strains could be related to the molecular characteristics of other individual junctional elements, including peripheral junctional components. Along these lines, preliminary analysis of the phosphate content of ZO-1 in filter-grown monolayers labeled to steady-state with [^{32}P]orthophosphate demonstrated that ZO-1 in the low resistance strain II contained approximately twice as much phosphate as that in the high resistance strain I (Stevenson, B. R., J. M. Anderson, I. D. Braun, and M. S. Mooseker, unpublished observations). Although this observed difference in phosphorylation state does not demonstrate a direct correlation between junctional permeability and ZO-1 phosphorylation, it does show that tight junctions which are indistinguishable by structural criteria can differ in the biochemical properties of junctional components.

We would like to express our gratitude to Deborah Braun and Deborah Sliker for their invaluable technical assistance; Michelle Peterson for her considerable grammatical skills; Jim Nelson for his assistance with the electrophysiology set-up; and Barry Gumbiner, Jim Madara, W. James Nelson, and Kai Simons for helpful discussions. As always, thanks to all the members of the Mooseker and Goodenough laboratories for their continuing support, patience, and friendship.

Work presented here was supported by grants from the National Institutes of Health to M. S. Mooseker (GM37556) and D. A. Goodenough (GM-28932), and Program Project Grant TO-1-DK38979, M. Kashgarian, P.I. J. M. Anderson is supported by a National Research Service Award (DK07864) and the Terry Kirgo Memorial Fellowship from the American Liver Foundation.

Received for publication 17 June 1988, and in revised form 27 September 1988.

References

1. Anderson, J. M., B. R. Stevenson, L. A. Jesaitis, D. A. Goodenough, and M. S. Mooseker. 1988. Characterization of ZO-1, a protein component of the tight junction from mouse liver and Madin-Darby canine kidney cells. *J. Cell Biol.* 106:1141–1149.
2. Bullivant, S. 1982. Tight junction structure and development. *In* The

Paracellular Pathway. S. E. Bradley and E. F. Purcell, editors. Josiah Macy, Jr. Foundation, New York. 13–35.
3. Cereijido, M., L. Gonzalez-Mariscal, G. Avila, and R. G. Contreras. 1988. Tight junctions. *CRC Crit. Rev. Anat. Sci.* 1:171–192.
4. Cereijido, M., E. S. Robbins, W. J. Dolan, C. A. Rotunno, and D. D. Sabatini. 1978. Polarized monolayers formed by epithelial cells on permeable and translucent support. *J. Cell Biol.* 77:853–880.
5. Cereijido, M., E. Stefani, and A. Martinez-Palomo. 1980. Occluding junctions in a cultured transporting epithelium: structural and functional heterogeneity. *J. Membr. Biol.* 53:19–32.
6. Citi, S., H. Sabanay, R. Jakes, B. Geiger, and J. Kendrick-Jones. 1988. Cingulin, a new peripheral component of tight junctions. *Nature (Lond.).* 333:272–276.
7. Claude, P. 1978. Morphological factors influencing transepithelial permeability: a model for the resistance of the zonula occludens. *J. Membr. Biol.* 39:219–232..
8. Claude, P., and D. A. Goodenough. 1973. Fracture faces of zonulae occludentes from "tight" and "leaky" epithelia. *J. Cell Biol.* 58:390–400.
9. Curci, S., and E. Fromter. 1979. Micropuncture of lateral intercellular spaces of Necturus gallbladder to determine space fluid K^+ concentration. *Nature (Lond.).* 278:355–357.
10. Diamond, J. 1977. The epithelial junction: bridge, gate, and fence. *Physiologist.* 20:10–18.
11. Farquhar, M. G., and G. E. Palade. 1963. Junctional complexes in various epithelia. *J. Cell Biol.* 17:375–412.
12. Frederikson, O., K. Mollgard, and J. Rostgaard. 1979. Lack of correlation between transepithelial transport capacity and paracellular pathway ultrastructure in Alcian Blue-treated rabbit gall bladders. *J. Cell Biol.* 80:383–393.
13. Fromter, E., and J. M. Diamond. 1972. Route of passive ion permeation in epithelia. *Nature (Lond.).* 235:9–13.
14. Fuller, S. D., and K. Simons. 1986. Transferrin receptor polarity and recycling accuracy in "tight" and "leaky" stains of Madin-Darby canine kidney cells. *J. Cell Biol.* 103:1767–1779.
15. Fuller, S., C.-H. von Bonsdorff, and K. Simons. 1984. Vesicular stomatitis virus infects and matures only through basolateral surface of the polarized epithelial cell line, MDCK. *Cell.* 38:65–77.
16. Deleted in proof.
17. Gonzalez-Mariscal, L., B. Chavez de Ramirez, and M. Cereijido. 1984. Effect of temperature on the occluding junctions of monolayers of epithelioid cells (MDCK). *J. Membr. Biol.* 79:175–184.
18. Gonzalez-Mariscal, L., B. Chavez de Ramirez, and M. Cereijido. 1985. Tight junction formation in cultured epithelial cells (MDCK). *J. Membr. Biol.* 86:113–125.
19. Goodenough, D. A., and J. P. Revel. 1970. A fine structural analysis of the intercellular junctions in mouse liver. *J. Cell Biol.* 45:272–290.
20. Gumbiner, B. 1987. The structure, biochemistry, and assembly of epithelial tight junctions. *Am. J. Physiol.* 253:C749–C758.
21. Gumbiner, B., and K. Simons. 1986. A functional assay for proteins involved in establishing an epithelial occluding barrier: identification of an uvomorulin-like polypeptide. *J. Cell Biol.* 102:457–468.
22. Kreutziger, G. O. 1968. Freeze-etching of intercellular junctions of mouse liver. *In* Proceedings of the 26th Annual Meeting of the Electron Microscopy Society of America. Claitor's Publishing Division, Baton Rouge, LA. 234–235.
23. Madara, J. L. 1987. Intestinal absorptive cell tight junctions are linked to cytoskeleton. *Am. J. Physiol.* 253:C171–C175.
24. Madara, J. L. 1988. Tight junction dynamics: is paracellular transport regulated? *Cell.* 53:497–498.
25. Madara, J. L., and K. Dharmsathaphorn. 1985. Occluding junction structure-function relationship in a cultured epithelial monolayer. *J. Cell Biol.* 101:2124–2133.
26. Madara, J. L., and J. R. Pappenheimer. 1987. Structural basis for physiological regulation of paracellular pathways in intestinal epithelia. *J. Membr. Biol.* 100:149–164.
27. Madara, J. L., and J. S. Trier. 1982. Structure and permeability of goblet cell tight junctions in rat small intestine. *J. Membr. Biol.* 66:145–157.
28. Madara, J. L., D. Barenberg, and S. Carlson. 1986. Effects of cytochalasin D on occluding junctions of intestinal absorptive cells: further evidence that the cytoskeleton may influence paracellular permeability and junctional charge selectivity. *J. Cell Biol.* 102:2125–2136.
29. Madara, J. L., R. Moore, and S. Carlson. 1987. Alteration of intestinal tight junction structure and permeability by cytoskeletal contraction. *Am. J. Physiol.* 253:C854–C861.
30. Marcial, M. A., S. L. Carlson, and J. L. Madara. 1984. Partitioning of paracellular conductance along the ileal crypt-villus axis: a hypothesis based on structural analysis with detailed consideration of tight junction structure-function relationships. *J. Membr. Biol.* 80:59–70.
31. Martinez-Palomo, A., and D. Erlij. 1975. Structure of tight junctions in epithelia with different permeability. *Proc. Natl. Acad. Sci. USA.* 72: 4487–4491.
32. Martinez-Palomo, A., I. Meza, G. Beaty, and M. Cereijido. 1980. Experimental modulation of occluding junctions in a cultured transporting epithelium. *J. Cell Biol.* 87:736–745.
33. Mollgard, K., D. N. Malinowski, and N. R. Saunders. 1976. Lack of correlation between tight junction morphology and permeability properties in developing choroid plexus. *Nature (Lond.).* 264:293–294.
34. Richardson, J. C. W., V. Scalera, and N. L. Simmons. 1981. Identification of two strains of MDCK cells which resemble separate nephron tubule segments. *Biochim. Biophys. Acta.* 673:26–36.
35. Rindler, M. J., I. E. Ivanov, and D. D. Sabatini. 1987. Microtubule-acting drugs lead to the nonpolarized delivery of the influenza hemaglutinin to the cell surface of polarized Madin-Darby canine kidney cells. *J. Cell Biol.* 104:231–241.
36. Simons, K., and S. D. Fuller. 1985. Cell surface polarity in epithelial cells. *Annu. Rev. Cell Biol.* 1:243–288.
37. Stevenson, B. R., and D. A. Goodenough. 1984. Zonulae occludentes in junctional complex-enriched fractions from mouse liver: preliminary morphological and biochemical characterization. *J. Cell Biol.* 98:1209–1221.
38. Stevenson, B. R., J. M. Anderson, and S. Bullivant. 1988. The epithelial tight junction: structure, function, and preliminary biochemical characterization. *Mol. Cell. Biochem.* 83:129–145.
39. Stevenson, B. R., J. D. Siliciano, M. S. Mooseker, and D. A. Goodenough. 1986. Identification of ZO-1: a high molecular weight polypeptide associated with the tight junction (zonula occludens) in a variety of epithelia. *J. Cell Biol.* 103:755–766.
40. van Meer, G., E. H. K. Stelzer, R. W. Wijnaendts-van-Resandt, and K. Simons. 1987. Sorting of sphingolipids in epithelial (Madin-Darby canine kidney) cells. *J. Cell Biol.* 105:1623–1635.